

Unsaturated poly(phosphoester)s *via* ring-opening metathesis polymerization†Cite this: *Polym. Chem.*, 2013, **4**, 3800Tobias Steinbach,<sup>abc</sup> Evandro M. Alexandrino<sup>b</sup> and Frederik R. Wurm<sup>\*b</sup>

For the first time, ring-opening metathesis polymerization of novel 7-membered cyclic phosphate monomers and their copolymerization with cyclooctene is presented. The monomers were investigated with respect to their metathesis behavior with different Grubbs catalysts and it was found that the Grubbs third generation catalyst gives the best results resulting in polymers with a molecular weight of up to 5000 g mol<sup>-1</sup>. Also copolymers with cyclooctene (up to a molecular weight of ca. 50 000 g mol<sup>-1</sup>) were synthesized and the monomer ratios were varied. The degree of polymerization could be controlled and the polydispersity index was usually below two. Acidic hydrolysis of the copolymer showed a complete shift of the molecular weight distribution to higher elution times in SEC, indicating a random incorporation into the poly(cyclooctene) backbone of the phosphate monomers and the possible degradation of the phosphate bonds along the backbone. Further, potentially degradable nanoparticles were prepared by a solvent evaporation miniemulsion technique.

Received 4th April 2013  
Accepted 23rd April 2013

DOI: 10.1039/c3py00437f

[www.rsc.org/polymers](http://www.rsc.org/polymers)

## Introduction

Degradable polymers are a growing field in modern materials science due to limitation of natural resources and due to the long half-life times of commodity plastics in nature.<sup>1</sup> Also for the biomedical field, for example as drug carriers, in tissue engineering or also when renal clearance of (macro)molecules is necessary, degradable – or partly degradable – polymers are of high interest.<sup>1,2</sup> Within the field of degradable polymers, polyesters are the most common materials with poly(lactide) probably being the most prominent example.<sup>2,3</sup> In recent projects, we have been focusing on the development of novel potentially biodegradable and biocompatible polyphosphoesters (PPEs).<sup>4</sup> PPEs can be degraded by several enzymes such as phosphatases and phosphodiesterases and/or by basic or acidic hydrolysis.<sup>5,6</sup> In spite of this obvious benefit, PPEs are only scarcely found in recent studies, even if they are easily accessible and allow the feasible synthesis of a great variety of (functional) materials.<sup>6</sup> In contrast polyesters based on carboxylic acids face the problem that functional cyclic lactones require multi-step syntheses or conventional polycondensation needs to be applied which also excludes many functional groups and limits the molecular

weight in many cases.<sup>7,8</sup> Almost 40 years ago, the group of Penczek developed the first strategies towards (mainly water-soluble) PPEs *via* polycondensation and ring-opening polymerization approaches.<sup>9,10</sup> These materials were not investigated in detail for at least two decades but can be found in modern literature in a few elegant reports in the fields of drug delivery or DNA transfection, for example.<sup>6</sup> We recently developed a route towards (un)saturated hydrophobic PPEs *via* acyclic diene metathesis polymerization (ADMET) of several phosphate monomers and we are currently investigating their performance in bioapplications.<sup>4</sup>

Some benefits of PPEs over conventional polyesters will be briefly mentioned here: (1) the additional functional group that is inherently brought in by the use of a pentavalent P-center (phosphorus triesters); (2) the high tendency to generate water-soluble polymers due to the hydrophilic phosphate building block; and (3) the general low degree of crystallinity (compared with highly crystalline materials such as PLA).

The combination of phosphorus chemistry with metathesis allows tailoring of the polymer functionality due to the high functional group tolerance of modern ruthenium metathesis catalysts and is currently under investigation in our group. Herein, we present an expansion of the metathesis polymerization towards PPEs from a step-growth acyclic diene metathesis (ADMET) polymerization to the chain-growth ring opening metathesis polymerization (ROMP).<sup>11</sup> We present different monomers, *i.e.* seven-membered cyclic phosphates, and their polymerization behavior is investigated. They are also copolymerized with *cis*-cyclooctene to yield high molecular weight polyesters with reasonable polydispersity. Further the copolymers were used in a miniemulsion solvent evaporation

<sup>a</sup>Institute of Organic Chemistry, Organic and Macromolecular Chemistry, Johannes Gutenberg-Universität Mainz (JGU), Duesbergweg 10-14, D-55128 Mainz, Germany

<sup>b</sup>Max-Planck Institute for Polymer Research (MPI-P), Ackermannweg 10, D-55128 Mainz, Germany. E-mail: wurm@mpip-mainz.mpg.de; Fax: +49 6131 370 330; Tel: +49 6131 379 723

<sup>c</sup>Graduate School Material Science in Mainz, Staudinger Weg 9, D-55128 Mainz, Germany

† Electronic supplementary information (ESI) available. See DOI: 10.1039/c3py00437f



process<sup>12,13</sup> to generate potentially biodegradable nanoparticles which can be used to encapsulate hydrophobic drugs or labels which are released slowly due to hydrolysis and enzymatic degradation.

## Results and discussion

### Monomer synthesis

For the synthesis of PPEs *via* ROMP, a cyclic phosphoester is mandatory. The smallest possible ring size is therefore a seven-membered ring that is readily available from *cis*-1,4-butenediol and phosphodichlorides. Due to the third phosphoester, a pendant group can be introduced prior to ring closure. Cyclic seven-membered phosphate monomers were synthesized by nucleophilic ring closing reaction of ethyl or phenyl dichlorophosphate with *cis*-1,4-butenediol. The reaction was carried out in a diluted THF solution (*ca.* 5 g L<sup>-1</sup>) with slow addition of the diol *via* a syringe pump over a period of 3–4 h to favor ring-closure over polycondensation (Scheme 1).

The crude reaction mixture was purified *via* silica gel chromatography to yield the desired unsaturated monomer in reasonable yields (higher than 60%) and high purity. Fig. 1 shows a representative <sup>1</sup>H NMR (400 MHz) spectrum of **2** in CDCl<sub>3</sub> (further characterization data can be found in the ESI, Fig. S1–S5†).

### Polymerization

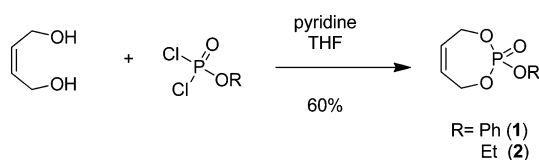
Monomers **1** and **2** were investigated with respect to their performance in ROMP. In a previous publication we have investigated the ADMET polymerization of several phosphate-

based monomers to high molecular weight unsaturated PPEs.<sup>4</sup> If diallyl-phenyl-phosphate was used as the respective monomer, no polymerization was observed. This was attributed to the negative neighboring group effect of the allylester that can complex the catalyst to form an inactive species for metathesis reactions<sup>14</sup> and indicated by a direct color change from purple to brown and not even oligomers were observed but only the intact monomer was recovered. When only one more methylene unit was incorporated, *i.e.* the dibutenyl ester, the polymerization proceeded under typical ADMET conditions.<sup>4,14</sup>

7-Membered cyclic monomers **1** and **2** presented herein resemble very closely these allyl esters after ring-opening, so their behavior in homopolymerizations was questionable but it was envisioned that metathesis could be more effective than the acyclic derivative due to the ring strain of an unsaturated seven-membered cyclic phosphate.

We carried out homopolymerizations of monomers **1** and **2** with the Grubbs 1<sup>st</sup> generation catalyst as the respective initiator (in solution, *r.t.*), but almost no polymerization was observed, only the presence of *ca.* 10–20% oligomers (*M<sub>n</sub>* < 1000 g mol<sup>-1</sup> from SEC, also compare <sup>1</sup>H NMR in the ESI†). When the same reaction was performed with the Grubbs 2<sup>nd</sup> generation catalyst, a slow polymerization was observed, but again without reaching 100% conversion. SEC proved a molecular weight of *ca.* 2000 g mol<sup>-1</sup> with a high PDI > 2 indicating transfer reactions and quenching of the active species which can be attributed to the allyl system complexing the catalyst as mentioned above. A similar behavior was reported for different seven-membered cyclodioxepins and cyclic amides (Scheme 2).<sup>15–17</sup>

When the Grubbs 3<sup>rd</sup> generation catalyst<sup>18</sup> was used under the same conditions, almost full monomer conversion for both monomers (**1** and **2**) was achieved (>90% from <sup>1</sup>H NMR). Fig. 2 shows the zoomed-in <sup>1</sup>H NMR spectra of polymerization mixtures of **2** with different catalysts. After ring-opening, the resonance for the methylene group of the ethyl side chain shifts to higher field (signal “c” in Fig. 1, from *ca.* 4.2 ppm in the



**Scheme 1** Synthetic approach to 7-membered unsaturated cyclic phosphates.

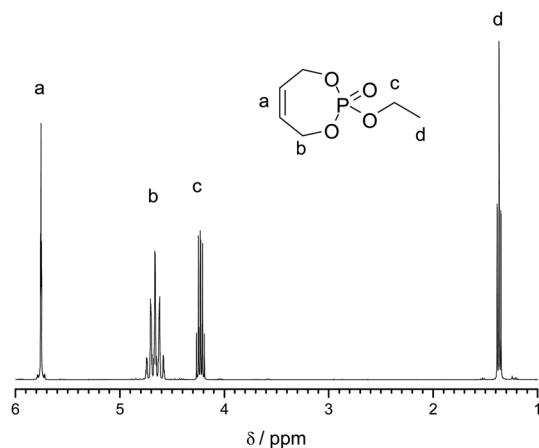
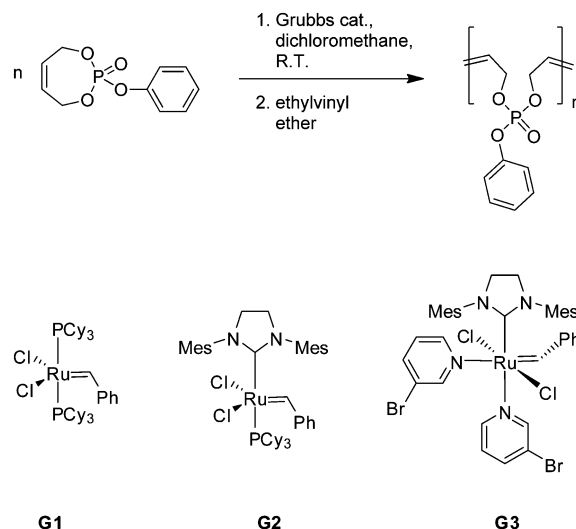


**Fig. 1** <sup>1</sup>H NMR (400 MHz) spectrum of **2** in CDCl<sub>3</sub>.



**Scheme 2** Ring-opening metathesis polymerization of **1** with different Grubbs-type catalysts.



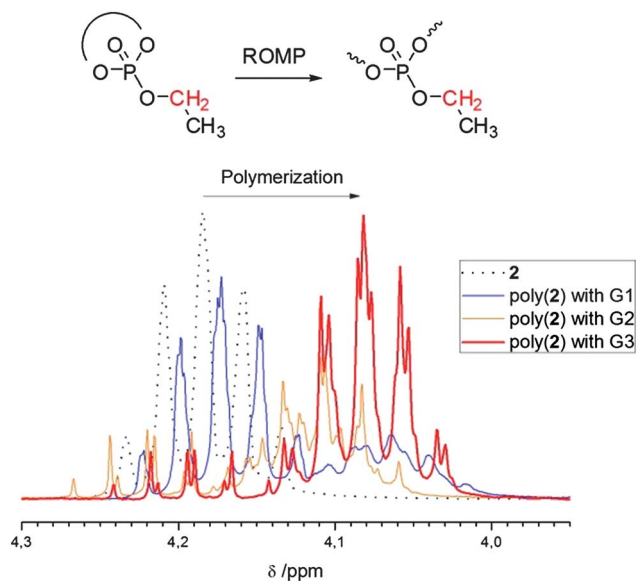


**Fig. 2** Zoom-in  $^1\text{H}$  NMR spectra of **2** and poly(**2**); the resonance of the methylene side chain shifts to higher field after ring-opening.

monomer to *ca.* 4.1 ppm in the polymer) and can be used to determine the degree of ring-opening, *i.e.* the monomer conversion. It can be clearly seen that only the Grubbs 3<sup>rd</sup> generation catalyst results in a reasonable degree of conversion. However, SEC elugrams still showed a broad molecular weight distribution ( $\text{PDI} = \text{ca. } 2$ ) and molecular weights usually lower than  $5000 \text{ g mol}^{-1}$ , which could not be increased by changing the catalyst : monomer ratio. This molecular weight limitation could be due to transfer or back biting reactions or catalyst deactivation by coordination (negative neighboring group effect)<sup>14</sup> which is currently under deeper investigation.

These results clearly demonstrate that the seven-membered unsaturated cyclic phosphates can be polymerized *via* ROMP, but that the polymerization is far from a living process; this further corroborates with recent results for analogue cyclic phosphoamidates, which were used to “terminate” a living ROMP of a norbornene polymerization (*i.e.* oligomerization at the chain end was observed).<sup>16</sup> The herein presented seven-membered cyclic phosphates could also be used as a second short block in other ROMPs yielding a terminal OH-group after acidic hydrolysis or enzymatic degradation; this is currently under investigation.

In the next experiments, the copolymerization of **1** and **2** with *cis*-cyclooctene (CO) as a comonomer was investigated.

To the best of our knowledge, there are no reports on the living polymerization of *cis*-cyclooctene primarily because

significant chain transfer from secondary metathesis of the unhindered polymer backbone occurs during ROMP, making it difficult to polymerize in a controlled fashion. This is due to the rather low ring strain of  $29 \text{ kJ mol}^{-1}$  of *cis*-cyclooctene,<sup>19</sup> which lowers its activity for living ROMP. However, the ROMP of CO and its derivatives represents a straightforward route towards linear polyolefins due to the availability of suitable starting materials and substantial ring strain of the eight-membered ring.<sup>20,21</sup> A copolymerization with the cyclic unsaturated phosphate presented herein should be feasible and was investigated in the following (Scheme 3). Table 1 lists all comonomer compositions and the molecular weights as well as thermal characterization.

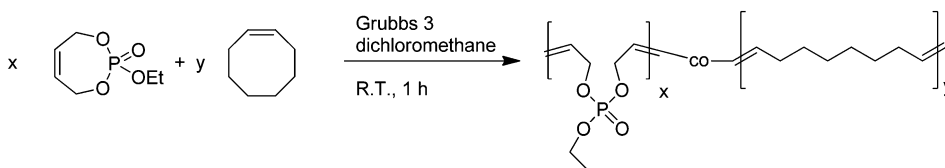
Different comonomer ratios were investigated and up to 30% phosphate monomer could be incorporated into the PCO backbone with a reasonable molecular weight (up to  $50\,000 \text{ g mol}^{-1}$ ) and molecular weight distribution (*ca.* 1.7–2) and full conversion. If higher amounts of phosphate monomer were used, incomplete conversion and broad molecular weight distributions were observed. The thermal properties of the copolymers were investigated by differential scanning calorimetry. With increasing degree of incorporation of the phosphate monomer, the melting temperature of PCO is lowered from *ca.*  $62 \text{ }^\circ\text{C}$  for pure PCO (with a molecular weight of  $30\,000 \text{ g mol}^{-1}$ ) to  $40 \text{ }^\circ\text{C}$  when 20% of **2** are copolymerized with CO. This is reasonable as the phosphate comonomers along the polymer backbone can be regarded as defects for the crystallization of PCO, thus lowering the melting points.

Fig. 3 shows an overlay of the  $^1\text{H}$  NMR spectra of the homopolymer of **2** (**P7**, top), the homopolymer of cyclooctene

**Table 1** Molecular characteristics of polyphosphoester-containing polymers prepared in this study

#	Monomer	Ratio C : P <sub>theo</sub> <sup>a</sup>	Ratio C : P <sub>NMR</sub> <sup>b</sup>	M <sub>n</sub> <sup>c</sup>	PDI <sup>c</sup>	T <sub>m</sub> <sup>d</sup>
<b>P1</b>	—	100	100	30 000	1.75	62
<b>P2</b>	<b>2</b>	9 : 1	10 : 1	43 200	1.72	55
<b>P3</b>	<b>2</b>	5 : 1	5 : 1	27 200	1.75	n.d.
<b>P3b</b>	<b>2</b>	5 : 1	5 : 1	41 100	1.75	45
<b>P4</b>	<b>2</b>	4 : 1	4 : 1	14 600	1.95	40
<b>P5</b>	<b>2</b>	7 : 3	9 : 3	18 700	1.87	n.d.
<b>P6</b>	<b>1</b>	0	0	2500	1.95	—*
<b>P7</b>	<b>2</b>	0	0	5500	1.90	—*
<b>P8</b>	<b>1</b>	8 : 2	8 : 2	40 000	1.90	54

<sup>a</sup> Monomer molar ratio between CO and **1** or **2**. <sup>b</sup> Molar ratio between CO and **1** or **2** determined from  $^1\text{H}$  NMR. <sup>c</sup> Number average of the molecular weight ( $\text{g mol}^{-1}$ ) and polydispersity index determined *via* SEC in chloroform *vs.* PS standards. <sup>d</sup> Melting points determined *via* differential scanning calorimetry (\* = no melting point observed).



**Scheme 3** Copolymerization of **2** with *cis*-cyclooctene.



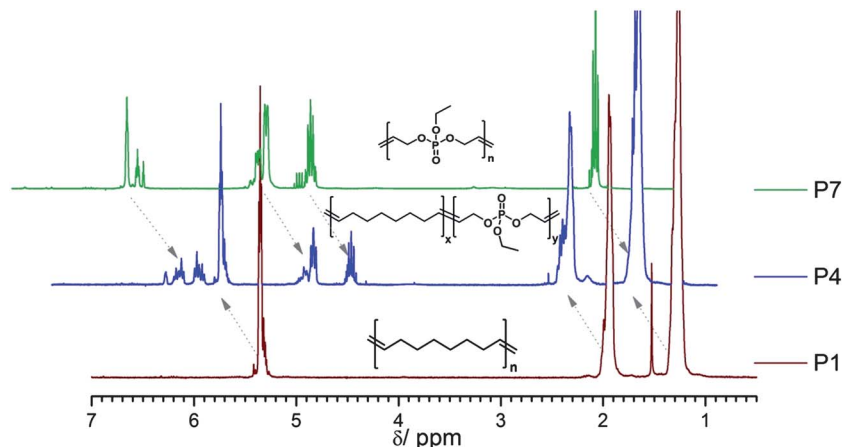


Fig. 3  $^1\text{H}$  NMR overlay (300 MHz in  $\text{CDCl}_3$ ): top, homopolymer of **2**; middle, copolymer of **2** and CO (ratio 1 : 4); bottom, homopolymer of CO.

(**P1**, bottom), and copolymer **P4** (with a theoretical ratio 4 : 1 = CO : 2). Clearly, the copolymer spectrum shows all resonances for PCO and P(2).

However, several other resonances can be detected. The appearance of different resonances for double bonds and methylene signals adjacent to them is expected due to the incorporation of both monomers in the polymer chain resulting in different dyad distributions. The signal pattern is similar to previously reported copolymers of CO and carborane-containing oxanorbornenes.<sup>22</sup> From detailed 2D NMR investigations of the P(PE-co-CO) copolymers (all spectra can be found in the ESI, Fig. S9–S11<sup>†</sup>) all additional signals could be assigned. Fig. S9<sup>†</sup> shows a representative TOCSY-H-NMR of polymer **P3** in  $\text{CDCl}_3$  (at 700 MHz). As expected for a ROMP, *cis* and *trans* double bonds (mainly *trans*) can be detected in the resulting polymers; for the PCO segments (also compare inset in Fig. S12<sup>†</sup>) these resonances are at 5.41 ppm for the *trans* and 5.37 ppm for the *cis*-oriented double bonds. Also the neighboring methylene units are affected by this orientation and two separate resonances can be detected at 1.4 and 1.3 ppm, respectively. In a CO-phosphate dyad the double bond signals shift downfield due to the proximity of the ester group to 5.8 and 5.6 ppm, respectively. For the very few double bonds between two phosphate units in the copolymer, their resonance can be detected at 5.95 ppm (lowest field due to the proximity to two ester groups). For the CP (or PC) and the PP dyad the methylene units next to the double bonds can also be distinguished at 4.6 and 4.5 ppm, respectively. The side chain ethyl group of the phosphate brings additional resonances at *ca.* 4.1 and 1.36 ppm. These signal assignments can be further verified by  $^1\text{H}$ - $^{31}\text{P}$  2D NMR (Fig. S11<sup>†</sup>). In a high resolution 700 MHz spectrum one can also detect the signals of the initiator (aromatic peaks at *ca.* 7.3 ppm) and the olefinic end group at *ca.* 6.2 ppm. The end groups are mainly attached to CO-units as a strong coupling to the methylene units in the aliphatic region can be detected but no coupling to phosphate-resonances (Fig. S12<sup>†</sup>). Fig. 4 summarizes the chemical shifts for the three different possible dyads.

**P2** ( $M_n$  43 200  $\text{g mol}^{-1}$ ) was subjected to an acidic hydrolysis with hydrochloric acid in THF. The resulting crude product was

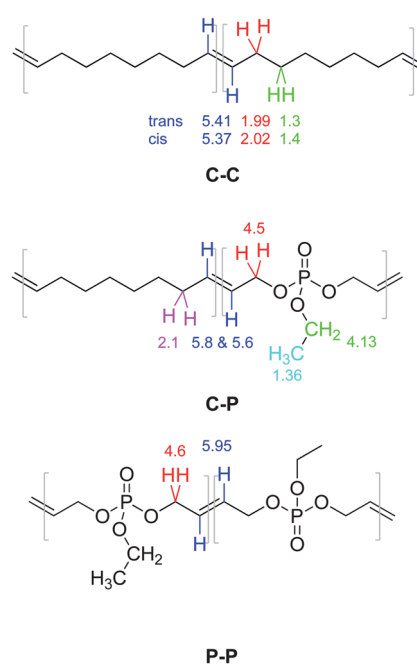


Fig. 4 Signal assignment of different resonances in the copolymer.

dried and the molecular weight was determined *via* SEC. Fig. 5 shows the respective molar mass distributions before and after hydrolysis proving a complete shift of the distribution to lower molecular weights indicating a rather random incorporation of **2** in the polymer backbone with an  $M_n$  of 4000  $\text{g mol}^{-1}$  after hydrolysis. These results further suggest the possibility of the hydrolytic or enzymatic degradation of the phosphoester bonds in possible (bio)applications.

As a potential application **P2** was exemplarily used in a solvent evaporation miniemulsion procedure to produce potentially biodegradable nanoparticles which could be used for the encapsulation of hydrophobic drugs.<sup>12,13,23</sup> Heterogeneous metathesis polymerization was previously used to prepare potentially biocompatible nanoparticles.<sup>23–25</sup> The polymer was dissolved in chloroform and dispersed in water



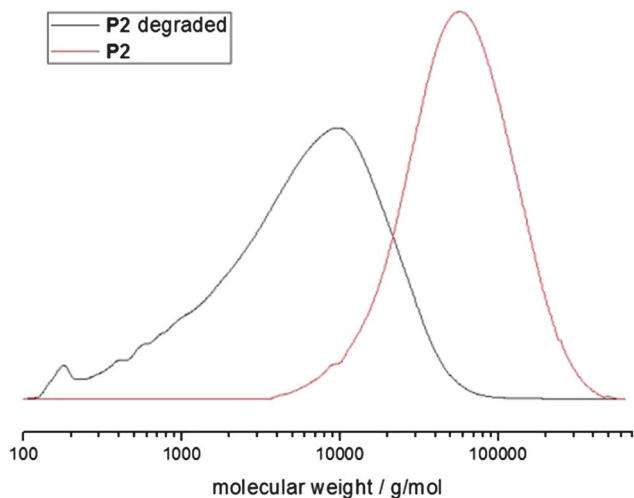


Fig. 5 Molecular weight distributions from SEC (in  $\text{CHCl}_3$ , vs. PS standards) of P2 and the hydrolyzed product.

containing SDS *via* ultrasound (for details compare the Experimental section) to generate a stable miniemulsion. Then the organic solvent was evaporated over a period of several hours to precipitate the polymer as a stable nanoparticle dispersion. Excess of surfactant was removed by dialysis and the particles were analyzed. By variation of the amount of surfactant and volume of the dispersed phase the particle size was varied. The hydrodynamic diameters of the particles in aqueous dispersion after dialysis were found to be 76 nm (procedure 1) and 140 nm (procedure 2) by dynamic light scattering. The stability of both systems was similar after the dialysis process with zeta-potential values of  $-49.2 \pm 11.7$  mV for the particles from procedure 1 and  $-65.2 \pm 5.7$  mV for the particles from procedure 2. Fig. 6 shows a representative SEM image of the particles (synthesized *via* procedure 2); the size distributions determined *via* dynamic light scattering can be found in the ESI (Fig. S14 and S15<sup>†</sup>). As

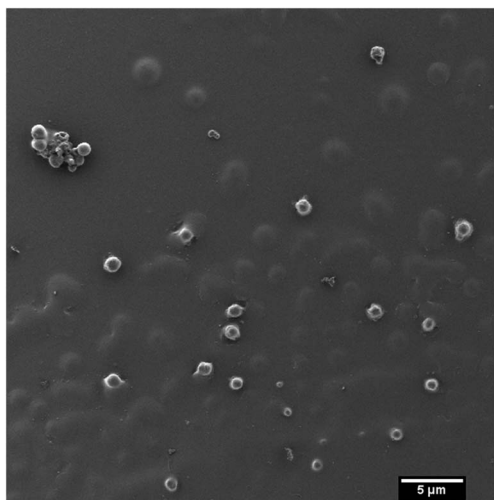


Fig. 6 Scanning electron micrographs of the nanoparticles obtained through the miniemulsion/solvent-evaporation approach using polymer P2.

expected, spherical particles were obtained. The size measured by SEM corresponds well to the values obtained from dynamic light scattering. As the polymer is rather soft (from DSC measurements) also the particles are soft and tend to agglomerate during the drying step.

## Experimental part

### Chemicals

All chemicals were purchased from Sigma Aldrich and used as received if not otherwise mentioned. Dichloromethane, tetrahydrofuran and triethylamine were dried and stored under argon. Grubbs catalyst 1<sup>st</sup> generation, Grubbs catalyst 2<sup>nd</sup> generation, and Grubbs catalyst 3<sup>rd</sup> generation were purchased from Sigma Aldrich and stored under argon.

### Instrumentation and methods

All the NMR experiments were carried out with a 5 mm BBI  $^1\text{H}/\text{X}$  z-gradient on a 700 MHz spectrometer with a Bruker Avance III system or on a Bruker AMX400. For  $^1\text{H}$  NMR spectra, 128 transients were used with an 11  $\mu\text{s}$  long  $90^\circ$  pulse and a 12 600 Hz spectral width together with a recycling delay of 5 s. The  $^{13}\text{C}$  NMR (176 MHz) and  $^{31}\text{P}$  NMR (283 MHz) measurements were carried out with an  $^1\text{H}$  powergate decoupling method using a  $30^\circ$  degree flip angle, which had a 14.5  $\mu\text{s}$  long  $90^\circ$  pulse for carbon and a 25.5  $\mu\text{s}$  long  $90^\circ$  pulse for phosphorus. The spectral widths were 41.660 Hz (236 ppm) for  $^{13}\text{C}$  and 56.818 Hz (200 ppm) for  $^{31}\text{P}$ , both nuclei with a relaxation delay of 2 s. The spectra of proton, carbon and phosphorus were recorded in  $\text{CDCl}_3$  at 298.3 K and were referenced as follows: for the residual  $\text{CHCl}_3$  at  $\delta$  ( $^1\text{H}$ ) = 7.26 ppm,  $\text{CDCl}_3$   $\delta$  ( $^{13}\text{C}$  triplet) = 77.0 ppm and triphenylphosphine (TPP)  $\delta$  ( $^{31}\text{P}$ ) = -6 ppm. The assignment was accomplished by the  $^1\text{H}, ^1\text{H}$  COSY (correlated spectroscopy) 2D method. The spectroscopic widths of the homonuclear 2D COSY experiments were typically 14 000 Hz in both dimensions (f1 and f2) and the relaxation delay was 1.2 s. The temperature was kept at 298.3 K and/or regulated by a standard  $^1\text{H}$  methanol NMR sample using the topspin 2.1 software (Bruker).

Size exclusion chromatography (SEC) measurements were carried out in  $\text{CHCl}_3$  consisting of a Waters 717 plus autosampler, a TSP Spectra Series P 100 pump, a set of three PSS SDV columns (104/500/50  $\text{\AA}$ ), and RI and UV (275 nm) detectors were used. Calibration was carried out using polystyrene standards provided by Polymer Standards Service. The glass transition temperature was measured by differential scanning calorimetry (DSC) on a Mettler Toledo DSC 823 calorimeter. Three scanning cycles of heating-cooling were performed (in a  $\text{N}_2$  atmosphere,  $30 \text{ mL min}^{-1}$ ) with a heating rate of  $10^\circ \text{C min}^{-1}$ .

The average particle size and particle size distribution were obtained by dynamic light scattering (DLS) in a submicron particle sizer NICOMP<sup>®</sup> 380, equipped with a detector to measure the scattered light at  $90^\circ$ .

The zeta-potential of the nanoparticle dispersion was measured using a Zetasizer NanoZ using an aqueous  $1 \times 10^{-3}$  M KCl solution as a dispersive phase.



The particle morphology characterization was carried out on a scanning electron microscope (SEM) Zeiss LEO Gemini 1530. The sample was drop cast in a silica slice and previously covered with a thin carbon coating layer using a coating system Leica EM MED020.

### Synthesis of 1 and 2

To a dried, two-necked 500 mL round bottom flask 2.4 g (11.4 mmol) of phenyl dichlorophosphate in the case of 1 (or 1.2 g (7.4 mmol) of ethyl dichlorophosphate in the case of 2) dissolved in 200 mL of dry THF, 8 eq. triethylamine was added with stirring under an argon atmosphere. The solution was cooled to 0 °C and then 1.1 equivalents of 1,4-*cis*-butenediol was added slowly (3–4 h) to the solution *via* a syringe pump in *ca.* 50 mL THF. The reaction was stirred overnight at room temperature. The crude mixture was concentrated, filtered and purified by silica chromatography to give a clear colorless liquid (for 1 : hexanes : acetone : ethyl acetate 4 : 2 : 1  $R_f$  = 0.5; for 2 : hexanes : acetone : ethyl acetate 2 : 2 : 1  $R_f$  = 0.55).

1: yield: 1.7 g (7.5 mmol, 66%).  $^1\text{H NMR}$  (300 MHz,  $\text{CDCl}_3$ ):  $\delta$  (ppm) = 4.78–4.69 (m, 4H ( $\text{CH}_2\text{-CH=CH-CH}_2\text{-O}$ )), 5.77 (m, 2H ( $\text{CH=CH}$ )), 7.25–7.13 (m, 5H, *Ph*).  $^{13}\text{C NMR}$  (75 MHz,  $\text{CDCl}_3$ ):  $\delta$  (ppm) = 64.7 ( $\text{CH}_2\text{-CH=CH-CH}_2\text{-O}$ ), 120 (arom), 125.3 (arom), 126.9 ( $\text{CH=CH}$ ), 129.8 (arom), 150.5 (arom).  $^{31}\text{P NMR}$  (162 MHz,  $\text{CDCl}_3$ ):  $\delta$  (ppm) = –2.04.

2: yield: 0.9 g (4.8 mmol, 68%).  $^1\text{H NMR}$  (300 MHz,  $\text{CDCl}_3$ ):  $\delta$  (ppm) = 1.33 (t, 3H ( $\text{O-CH}_2\text{-CH}_3$ )),  $^3J$  = 6.0 Hz, 4.18 (m, 2H ( $\text{O-CH}_2\text{-CH}_3$ )), 4.63 (m, 4H ( $\text{CH}_2\text{-CH=CH-CH}_2\text{-O}$ )), 5.70 (m, 2H ( $\text{CH=CH}$ )).  $^{13}\text{C NMR}$  (75 MHz,  $\text{CDCl}_3$ ):  $\delta$  (ppm) = 16.2 ( $\text{O-CH}_2\text{-CH}_3$ ), 64.1 ( $\text{CH}_2\text{-CH=CH-CH}_2\text{-O}$ ), 64.5 ( $\text{O-CH}_2\text{-CH}_3$ ), 127.1 ( $\text{CH=CH}$ ).  $^{31}\text{P NMR}$  (162 MHz,  $\text{CDCl}_3$ ):  $\delta$  (ppm) = 3.78.

### Representative procedure for ROMP

In a glass tube the monomers were dissolved in dry dichloromethane (100 mg of monomers in 2 mL of solvent) and the appropriate catalyst was added as a solution (*ca.* 5 mg (depending on the targeted molecular weight) in 100  $\mu\text{L}$  dichloromethane) to the vigorously stirred mixture under an argon atmosphere. The reaction was stirred for 1 h, then 100  $\mu\text{L}$  of ethyl vinyl ether was added to terminate the active chain end, concentrated *in vacuo* and precipitated in diethyl ether. The polymers were then dissolved in  $\text{CH}_2\text{Cl}_2$ , treated with activated charcoal and filtered over celite. They were isolated and then precipitated from methylene chloride into diethyl ether and finally dried. Yields are usually 80–90%.

### Procedure for nanoparticle preparation

30 mg of polymer P2 was dissolved in 1.25 g (procedure 1) or 0.62 g (procedure 2) of chloroform. 5 mL of Milli-Q water containing 10 mg (procedure 1) or 5 mg (procedure 2) of sodium dodecyl sulfate were added to the chloroform solution and stirred over a period of 60 min for the formation of the pre-emulsion. Then, the pre-emulsion was subjected to a pulsed ultrasonication process under an ice bath for 120 s (30 s sonication and 10 s pause) at 70% amplitude in a ¼" tip Brason 450 W sonifier. The obtained miniemulsion was kept at 30 °C in an

oil bath over a period of 8 h to completely evaporate the organic solvent. The obtained nanoparticle dispersion was further purified by exhaustive dialysis against water for approximately 15 h before being used for further studies.

### Conclusion

In summary we were able to synthesize novel seven-membered cyclic phosphates which can be applied to the synthesis of degradable PPEs and copolymers with cyclooctene *via* ROMP. Molecular weights and comonomer ratios can be controlled by the catalyst : monomer ratio as ruthenium alkylidene is acting as the initiator. This paper is the first report for the synthesis of polyphosphoesters *via* ROMP. This broadens the field of biodegradable polyesters and we believe that with this approach, the previously established step growth ADMET protocol can be extended to a chain growth polymerization strategy and will allow us to synthesize telechelic materials and copolymers with other typical ROMP-monomers, for example norbornene-derivatives. We have also demonstrated with a simple approach that potentially biodegradable nanoparticles with different particle sizes and size distributions can be produced from these new polyesters, which can be an interesting option for future applications in the development of drug delivery systems, particularly for hydrophobic drugs.

### Acknowledgements

T.S. is grateful to the Max Planck Graduate Center with the Johannes Gutenberg-Universität Mainz (MPGC) for a fellowship and financial support. T.S. is a recipient of a fellowship through funding of the Excellence Initiative (DFG/GSC 266) in the context of the graduate school of excellence "MAINZ" (Materials Science in Mainz). E.M.A. is grateful to the International Max-Planck Research School (IMPRS) for a fellowship. F.W. thanks the Alexander-von-Humboldt foundation for financial support.

### References

- 1 A. A. Shah, F. Hasan, A. Hameed and S. Ahmed, *Biotechnol. Adv.*, 2008, **26**, 246–265.
- 2 L. S. Nair and C. T. Laurencin, *Prog. Polym. Sci.*, 2007, **32**, 762–798.
- 3 R. Mehta, V. Kumar, H. Bhunia and S. N. Upadhyay, *J. Macromol. Sci., Part A: Pure Appl. Chem.*, 2005, **45**, 325–349.
- 4 F. Marsico, M. Wagner, K. Landfester and F. R. Wurm, *Macromolecules*, 2012, **45**, 8511–8518.
- 5 H. Q. Mao and K. W. Leong, in *Advances in Genetics*, ed. M.-C. H. Leaf Huang and W. Ernst, Academic Press, 2005, vol. 53, pp. 275–306.
- 6 S.-W. Huang and R.-X. Zhuo, *Phosphorus, Sulfur, and Silicon and the Related Elements*, 2008, **183**, 340–348.
- 7 M. Trollsås, V. Y. Lee, D. Mecerreyes, P. Löwenhielm, M. Möller, R. D. Miller and J. L. Hedrick, *Macromolecules*, 2000, **33**, 4619–4627.
- 8 S. Ji, B. Bruchmann, F. Wurm and H.-A. Klok, *J. Polym. Sci., Part A: Polym. Chem.*, 2012, **50**, 25–34.



- 9 G. Lapienis and S. Penczek, *Macromolecules*, 1974, **7**, 166–174.
- 10 S. Penczek, J. Pretula and K. Kaluzynski, *Biomacromolecules*, 2005, **6**, 547–551.
- 11 C. W. Bielawski and R. H. Grubbs, *Prog. Polym. Sci.*, 2007, **32**, 1–29.
- 12 A. Musyanovych, J. Schmitz-Wienke, V. Mailänder, P. Walther and K. Landfester, *Macromol. Biosci.*, 2008, **8**, 127–139.
- 13 M. Urban, A. Musyanovych and K. Landfester, *Macromol. Chem. Phys.*, 2009, **210**, 961–970.
- 14 K. B. Wagener, K. Brzezinska, J. D. Anderson, T. R. Younkin, K. Steppe and W. DeBoer, *Macromolecules*, 1997, **30**, 7363–7369.
- 15 S. Hilf, R. H. Grubbs and A. F. M. Kilbinger, *Macromolecules*, 2008, **41**, 6006–6011.
- 16 A. A. Nagarkar, A. Crochet, K. M. Fromm and A. F. M. Kilbinger, *Macromolecules*, 2012, **45**, 4447–4453.
- 17 S. Hilf, E. Berger-Nicoletti, R. H. Grubbs and A. F. M. Kilbinger, *Angew. Chem. Int. Ed.*, 2006, **45**, 8045–8048.
- 18 T.-L. Choi and R. H. Grubbs, *Angew. Chem.*, 2003, **115**, 1785–1788.
- 19 P. v. R. Schleyer, J. E. Williams and K. R. Blanchard, *J. Am. Chem. Soc.*, 1970, **92**, 2377–2386.
- 20 J. Alonso-Villanueva, J. M. Cuevas, J. M. Laza, J. L. Vilas and L. M. León, *J. Appl. Polym. Sci.*, 2010, **115**, 2440–2447.
- 21 C. Liu, S. B. Chun, P. T. Mather, L. Zheng, E. H. Haley and E. B. Coughlin, *Macromolecules*, 2002, **35**, 9868–9874.
- 22 Y. C. Simon and E. B. Coughlin, *J. Polym. Sci., Part A: Polym. Chem.*, 2010, **48**, 2557–2563.
- 23 L. Pichavant, C. Bourget, M.-C. Durrieu and V. Héroguez, *Macromolecules*, 2011, **44**, 7879–7887.
- 24 C. Airaud, E. Ibarboure, C. Gaillard and V. Héroguez, *J. Polym. Sci., Part A: Polym. Chem.*, 2009, **47**, 4014–4027.
- 25 D. Le, V. Montembault, S. Pascual, F. Collette, V. Héroguez and L. Fontaine, *Polym. Chem.*, 2013, **4**, 2168–2173.

